International Journal of Science and Research (IJSR)
ISSN (Online): 2319-7064
Index Copernicus Value (2013): 6.14 | Impact Factor (2015): 6.391

"Land Use/Land Cover Status relating the Coal fire of Jharia Coal Field" - An Analytical Case Study by RS-GIS Techniques

Goutam Das[1], Rabin Das[2]

Research Fellow, Visva Bharati University & 2. Asst. Professor of Geography, Bajkul Milani Mahavidyalaya (VU)

Abstract: ***Jharia coal mines are India's most important storehouse of prime coke coal used in blast furnaces; it consists of 23 large underground and nine large open cast mines. The mining activities in these coalfields started in 1894 and had really intensified in 1925. Jharia is famous for a coal field fire that has burned underground for nearly a century. The first fire was detected in 1916. The rapid and extensive underground and opencast mining is going on continuously in an area like the Jharia Coal Field (JCF), where temperature and land-use studies are of paramount importance. Remote sensing and GIS techniques have been used to identify the action of different NDVI, temperature, land-use classes on satellite imagery and enhanced products and identify the action of time-sequential changes in temperature and land-use patterns that have occurred in the JCF since 2001 June and particularly between to June 2011 have been investigated. The different temperature and land-use classes, recognized from satellite image data and field surveys, are Settlement, Barren Land, agricultural land, Scrub land, vegetation, river sand, mining area, and fellow land. A number of image processing operations have been carried out on remote sensing data for enhancing NDVI patterns. It has been found that Landsat TM, ETM+ false color composites (FCC) of bands 4, 3 and 2; FCC of bands 7, 5 and 3; FCC of bands 5, 4 and 3 and ratio images provide very useful information for land-use mapping. The Normalized Difference Vegetation Index (NDVI) images have been used for vegetation studies and deference land surface temperature. So, magnitude of the mining area is rapidly increasing day to day on temporal scale and total increase in mining from 2001 to 2011 is 4.85%.Temperature and Land-use changes have been detected by image differencing, rationing and of NDVI images. In the year 2001, the eastern part of the Jharia coal field was more affected by coal fire than the western part. Hence, the eastern part is always affected by the coal fire. An increase (1.67 km2) in the total coal-fire area was observed from 2001 to 2011. There are some human settlements present close to mining and fire-affected areas. That is extensive mining area , establishment of communication networks, expansion of settlements and decrease in the vegetation cover area etc., have remodeled the face of the JCF of is inferred from the remote sensing images.***

Keywords: opencast mining, Remote Sensing and GIS, Coal Fire Map, NDVI, Surface Temperature Map, Land-use changes

1. Introduction

Jharia is a notified area and one of eight development blocks of Dhanbad district in Jharkhand state, India. Jharia is famous for its rich coal resources, used to make coke. Jharia plays a very important role in the economy and development of Dhanbad City, and can be considered as a part of Dhanbad City. The coal field lies in the Damodar River Valley covering about 110 square miles (280 square km) and produces bituminous coal suitable for coke and most of India's coal comes from Jharia. But, its surface and subsurface coal fire is the major problem here like many coal producing countries as China, Australia, India etc. Coal fire results from man-made activities, accident, forest/bush fire, lighting strike etc. Today coal burns more than 152 meters underground, and is still slowly spreading in the coal seam. In India, at Jharia some of the subsurface coal fires have already been burning over many decades, and now they are spreading caused by mining introduced spontaneous combustion (Mukherjee et al. 1991, sinha 1989). Coal fire is main cause of Jharia that has burned underground coal for nearly a century. The first fire was detected in 1916. In 1972, more than 70 mine fires were reported in this region and as report of 2010, 68 fires were burning beneath a 58-square-mile (150 km2) region of the Jharia coalfield (JCF), this field was only major source of coke coal.

2. The Study Area

The sickle-shaped Jharia coal field (JCF) is situated in Dhanbad district of Jharkhand and located about 250km northwest of Kolkata. The JCF is bounded by 23º37´N to 23º50´N latitude and 86º8´E to 86º30´E longitude with an area 700 km2. The Jharia coal field is the major source of coke coal, produce 80% coke coal all over India. Major part of this area is influenced by The Damodar River.

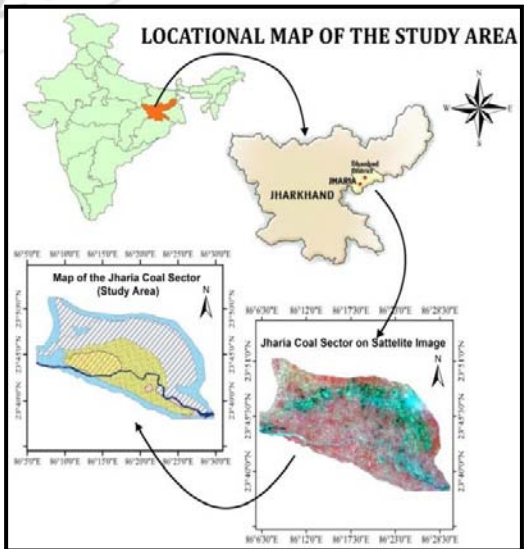

Figure 1: Location Map of the Study Area

3. Geology

Rocks of Jharia coal field belonging to the Gondwana Super group from Upper Carboniferous to Lower Cretaceous age. The rocks are older from 320 to 98 million years. the area is underlain by unconformably Archaean metamorphics, Mainly composed of sedimentary rocks of the Permian period . The rocks of the Gondwana Supergroup, the Permian Barakar and Raniganj formations have been more potential for coal production in comparison to other formations.

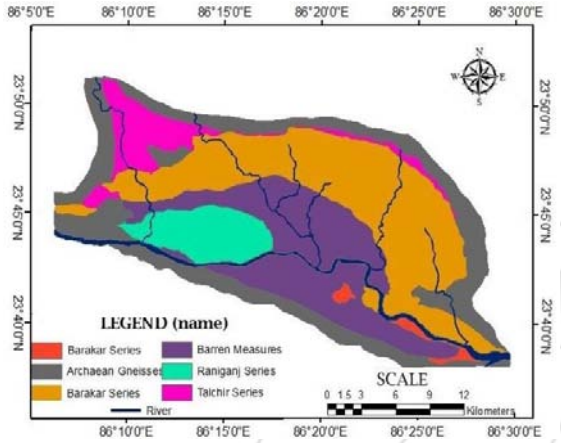

Figure 2: Geological Map of the Study Area

Most of the coal mines in this area are present in the Barakar Formation, which consists of coarse to medium grey and white sandstones, shales and coal seams. Raniganj consists of grey and greenish soft feldspathic sandstones, shales and coal seams (T. R. Martha et al. 2008). There are 28 major coal seams in Jharia, 19 in the Barakar formation (the older stratigraphic horizon) and 9 in the Raniganj formation (the younger stratigraphic horizon). The thickness of the Barakar formation is 0.9–22.0 m and the coal to non-coal ratio is 1:2.5; the thickness of the Raniganj formation is 0.9–3.7 m and the coal to non-coal ratio is 1:39.0. The average thickness of coal seams in this coalfield varies from 3 to 5 m. (P. K. Gangopadhyay et al. 2008). A recent Geographical Survey of India (GSI) report suggests that Jharia coalfield has total reserves of coal of 19.4 billion tones (103 kg) (GSI 2004).

4. Physiography

Jharia coal field represents more or less flat topography with an average height of 160Mt. above mean sea level. The maximum and minimum elevation is 220Mt & 77Mt. respectively Jharia coalfield is characterized by gently undulating to a rolling topography with an overall slope towards east-southeast. The coalield is roughly sickle shaped on plan and occurs as a basin with its axis trending broadly east-west and plunging towards the west. The southern flank is truncated by a major Boundary Fault. The general dip of the formation is 10 to 15 degrees. Flatter dips have also been noted at places. The entire southern part of Jharia coalfield in the vicinity of the Boundary Fault, however shows generally steep dipping beds with amounts increasing even up to 70 degrees (Coal India Limited, 2010).

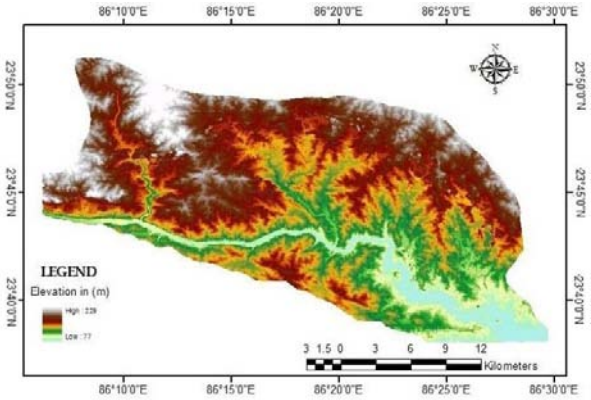

Figure 3: Digital Elevation Model of Jharia coal field

5. Drainage

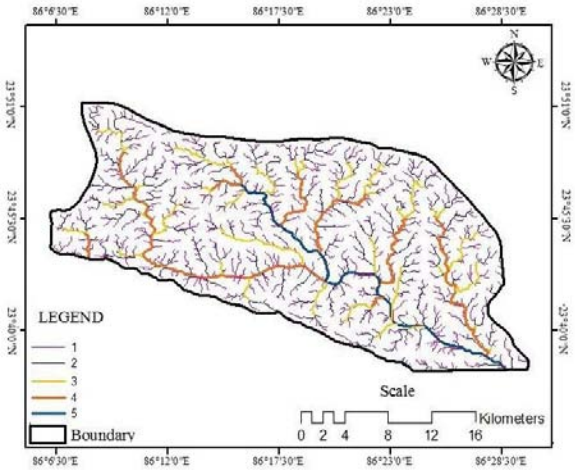

Figure-4: Drainage Map of Jharia coal field

Drainage pattern of an area is very important in terms of its groundwater potentiality. It is the source of surface water and is affected by structural, lithological and geomorphological control of an area (Schumm, 1956).The drainage pattern in the Jharia coalfield is dendritic in nature. This may be due to more or less homogeneous lithology and structural controls. Damodar River is the main control of drainage system along the Jharia coalfield. It is a fourth order stream to which a number of third to first order streams, viz. Jamunia, Khudia, Katri, Ekra, Tisra, Chatkari etc. join. Damodar River flows along the southern periphery of the coalfield and is guided by the Great Boundary Fault. The main flow direction is from west to east.

a) Vegetation:

Vegetation cover in the coalfield area has been found to be predominantly of five classes.

- Dense Forest.
- Open Forest.
- Scrubs.
- Plantation on Over Burden (OB) Dumps / Backfilled area, and
- Social Forestry.

According to report of Coal India Limited, 2008 total vegetation cover is 170.53 sq. Km(forest land, scrubs land, plantation covers 8.82 sq. Km, 133.46 sq. Km, 23.84 sq. Km

respectively) is Jharia coal fire. Various vegetation species present in this study area.

b) Climate

Climatically this area is sub humid and tropical which has three seasons e.g., summer, rainy and winter in succession. The annual rainfall is 120 mm (2010) and means annual temperature is around 27.7°C. Maximum temperature often goes over 40°C in summer season and minimum temperature often goes below 10°C in winter season. Average temperature in summer season is 34°C and cold season is 18°C.

c) Objectives of the study:

- Identification of coal fire zone using Geo-informatics in Jharia coal field. The main objective of this study includes-
- Delineate coal mining areas using satellite data.
- Detection of coal fires through the use of temporal satellite data.
- Coal fires related land use & land cover change

d) Methodology and data collection

Detection of Coal fires and identification land use change in Jharia coal field using Landsat satellite image. Used temperature mapping algorithm for detection coal fire and Land use & land cover classification have been done using maximum likelihood classification technique. Different image processing & enhancement technique used for identification the time-sequential changes in land use parrens.

The data used for this dissertation consists of:

1) Landsat7 ETM+ imagery, from band 1to band 7, and a panchromatic image on23rd August, 1999.
2) Landsat5 TM imagery, from band1 to band 7 on 10th November, 1992 & 1st November, 2010.
3) Digital elevation model of 2010.
4) Geological map of 1930(after fox 1930).
5) Scanned topographical map, scale of 1:100.000.

Some data, as Landsat TM &ETM+ images, free data collected from USGS web site. Entire study area, we used Landsat-TM & ETM+ images (path-139 & row-40). For temperature mapping used band-6, which cover thermal region (8µm-13µm) of electromagnetic spectrum (EMS). Spatial resolution of thermal band of Landsat-TM & Landsat-ETM+ is 120m and 60m respectively and spectral resolution of visible, infrared & middle infrared region of Landsat-TM & ETM+ is 30m. Due its moderate resolution spatial coverage, Land use & land cover classification has been done for change detection analysis. Panchromatic image of Landsat-7, spatial resolution is 15m, help for LULC classification.

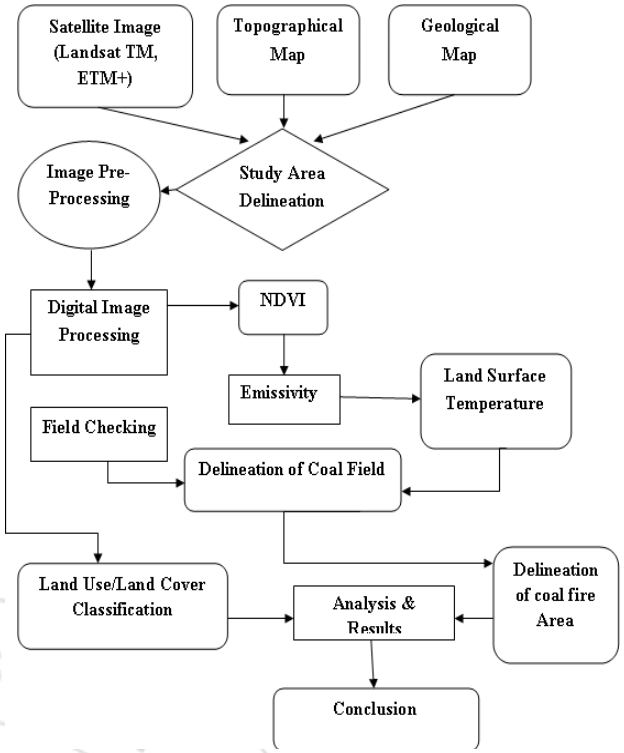

Figure 5: Flow Chart including different methods for Study

e) Instruments Used:

Garmin GPS 12: GPS was used to obtain the geographical co-ordinates of the observed filed location during the ground truth study for collecting coal fires, coal zone & land use/land cover information.

f) Methodology:

Remote sensing is the time consuming & low cost modern technique for identify various geo-hazard like Coal fires etc. In order to identify the thermal anomalies related to coal fire through the help of remote sensing. After identify coal fires zone & coal mine we analyze how affect coal fire on various land scape.This dissertation work is divided into three steps. The first step is related to data collection and image pre-processing. Secondly, to detect coal fires by means of feature extraction with the help of image processing techniques. The last step is conformation step using field data and other related information.

g) Surface temperature monitoring using Remote Sensing in JCF:

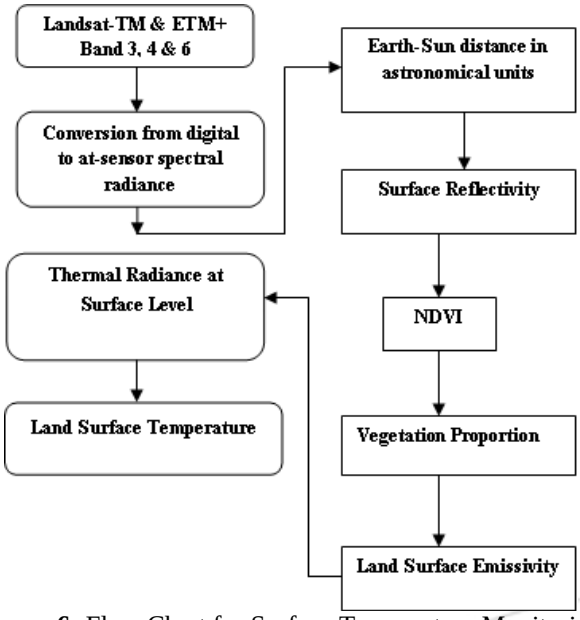

Figure 6: Flow Chart for Surface Temperature Monitoring

Land surface temperature (LST) is an important parameter for formulating surface– atmosphere interactions (Dickinson 1996, Sobrino et al. 2003a, b, 2004). Surface temperature of the earth surface depends on rocks, soil, vegetation cover, land use patterns and local climate. In this paper major work is coal fires detection, which work is done with help of land surface temperature estimation. The Atmospherically corrected red band & infrared band use for NDVI calculation to extract surface emissivity. Through the help of Erdas Community & SEBAL model and using NDVI, emissivity & thermal band make a temperature mapping algorithm of Landsat-TM & ETM+ sensors images.

h) Principle of coal fire mapping trough help of remote sensing:

All objects having temperature above absolute zero (o k or -273 ºc) continuously emits EMR. In thermal remote sensing, sensors record this emitted or radiated or radiated energy instead of reflected energy. Therefore, in thermal remote sensing, the object itself is the source of energy.Although real objects do not behave as black bodies, this concept of blackbody is a convenient theoretical vehicle to describe the radiation principles of a material. The amount of radiation of a blackbody differs with the change of wavelength and its kinetic temperature. The amount of energy in object radiates in per unit area (considering all wavelengths) can be expressed by Stefan- Boltzmann law-

$$M=€T4 \quad \ldots\ldots (1)$$

Where,
M= total radiant existence from the surface of a material, measured in W/ M2.
€=Stefan-Boltzmann constant=5.6697*10-8 W/m2/K4.
T= Temperature of emitting body, measured in K.

The above equation tells us that doubling the absolute temperature of a body would render 16 times more radiation. The wavelength in which the maximum energy will be radiated or emitted is given by Wien‟s displacement law-

$$€MAX=b/T \quad \ldots\ldots (2)$$

Where,
€MAX= wavelength of maximum emitted energy, measured in µm.
b = Wien‟s displacement constant= 2.897.7685 µm K
T = temperature of emitted body, measured in K.

According to this law, for the sun, with a temperature of about 6000 K, the peak radiation is at 0.58 µm the objects over the earth, as observed from, have peak radiation within 8-14 µm regions. In 1990, Max Planck published a paper on the thermal properties of blackbodies that become one of the foundation stones from which quantum physics was built on. The plank blackbody radiation law gives the rate at which blackbody objects radiate thermal energy. Depending on what terms (parameters) and unit systems are used, the Planck equation can be written in various ways. One such form is as follows-

$$E(\lambda T) = \frac{2\pi hc^2}{\pi s\left(\frac{hc}{e\lambda kt}-1\right)} \quad \ldots\ldots (3)$$

Where,
E = blackbody spectral radiance, measured in W/m/m.
= wavelength, measured in m
c= speed of light = 2.998 * 108 m/s
h= plank‟s constant = 6.626 * 10-23 J/K
T= temperature of blackbody, measured in K
e= base in natural algorithm = 2.71828
Equation (3) can be rearranged as follows (T. R. Martha et al. 2008)

$$Trad = c2/[\lambda In\left\{\left(\frac{Ec\,1\lambda 5}{\pi L\lambda}\right)+1\right\}] \quad \ldots\ldots (4)$$

Where,
Trad = radiant temperature in K,
C1 =2πhc2=3.742* 10-16 w/m-2
C2 = hc/k = 0.0144 Mk
E= emissivity

Landsat-TM & ETM+ Data Processing for Land surface Temperature Estimation:

Spectral Radiance:

Firstly, the digital number (DN) of band 3, 4 and 6 were converted to space reaching radiance or top-of-atmospheric (TOA) radiance (at-sensor spectral radiance) by using the equation 1. (Markham and Baker 1986)

Lλ=(LMAX-LMIN/QCALMAX-QCALMIN)× (QCAL-QCALMIN)+LMIN……..(5)

Where,
Lλ= spectral radiance at the sensor aperture in watts/ (meter2 *ster* µ m),
QCAL= the quantized calibrated pixel value in DN,
LMIN= the spectral radiance that is scaled QCALMIN to in watts/(meter2 *ster* µ m),
LMAX= the spectral radiance that is scaled to QCALMAX in watts/(meter2 *ster* µ m),
QCALMIN= the minimum quantized calibrated pixel value (corresponding to LMIN) in DN,
QCALMAX= the maximum quantized calibrated pixel value (corresponding to LMAX) In DN.
LMAX and LMIN are the spectral radiances for each band at digital number 1 and 255 (i.e.QCALMIN, QCALMAX), respectively.

Reflectivity (Pλ):
Reflectivity is the fraction of incident radiation reflected by a surface. In general it must be treated as a directional property that is a function of the reflected direction, the incident direction, and the incident wavelength. Reflectivity is distinguished from reflectance by the fact that reflectivity is a value that applies to thick reflecting objects. When reflection occurs from thin layers of material, internal reflection effects can cause the reflectance to vary with surface thickness. Reflectivity is the limit value of reflectance as the surface becomes thick; it is the intrinsic reflectance of the surface, hence irrespective of other parameters such as the reflectance of the rear surface. Another way to interpret this is that the reflectance is the fraction of electromagnetic power reflected from a specific sample, while reflectivity is a property of the material itself, which would be measured on a perfect machine if the material filled half of all space.

The reflectivity for each band (ρλ) is defined as the ratio of the reflected radiation flux to the incident radiation flux. It is computed using the following equation given for Landsat images:

$$P\lambda = \frac{\pi \quad \lambda}{ESUN\ \lambda \qquad \text{ø} \quad dr} \ldots\ldots\ldots\ldots\ldots\ldots\ldots\ldots (6)$$

Where, Lλ = spectral radiance for each band (calculated in equation-5),
ESUNλ= mean solar exo-atmospheric irradiance for each band (W/m2/µm)
□□□ø =Cosine of the solar incidence angle (from nadir),
d_r=Inverse squared relative earth-sun distance. So, Pλ is calculated following steps,
□□□ø =Cosine of the solar incidence angle (from nadir),
Cosine θ is computed using the header file data on sun elevation angle (β) where,
θ= (900- β), Where, β= sun elevation angle.

The header file of study area is seen sun elevation angle (β)=46.3137769 & 45.30147378 in 2001.11.02 & 2011.11.06 respectively.
So, ø=(900- β), ø=(900-46.3137769),
= 43.6862231 (for 2001.11.02)
= 44.69852622 (for 2011.11.06)

Inverse Squared Relative Earth-Sun Distance (dr):
The term dr is defined as 1/de-s2 where de-s is the relative distance between the earth and the sun in astronomical units. dr is computed using the following equation by Duffle and Beckman (1980)1, also given in FAO 56 paper: Crop Evapotranspiration (Allen et al., 1998):

$$dr = 1 + 0.033\cos\left(DOY\ \frac{2\pi}{365}\right)$$

DOY=Sequential day of the year and the angle (DOY × 2π/365) is in radians. Values for dr range from 0.97 to 1.03 and are dimensionless.

$$Dr = 1 + 0.033\cos DOY\frac{2\pi}{365},$$

= 1+0.033cos (3062π/365) (2001.11.02)
. 1.032985403
= 1+0.033cos (3062π/365) (2011.11.06)
=1.029869974

Spectral Radiance
Firstly, the digital number (DN) of band 3, 4 and 6 were converted to space reaching radiance or top-of-atmospheric (TOA) radiance (at-sensor spectral radiance) by using the equation 1. (Markham and Baker 1986)

Reflectivity (P)
Reflectivity is the fraction of incident radiation reflected by a surface. In general it must be treated as a directional property that is a function of the reflected direction, the incident direction, and the incident wavelength. Reflectivity is distinguished from reflectance by the fact that reflectivity is a value that applies to thick reflecting objects. When reflection occurs from thin layers of material, internal reflection effects can cause the reflectance to vary with surface thickness. Reflectivity is the limit value of reflectance as the surface becomes thick; it is the intrinsic reflectance of the surface, hence irrespective of other parameters such as the reflectance of the rear surface. Another way to interpret this is that the reflectance is the fraction of electromagnetic power reflected from a specific sample, while reflectivity is a property of the material itself, which would be measured on a perfect machine if the material filled half of all space. The reflectivity for each band (ρλ) is defined as the ratio of the reflected radiation flux to the incident radiation flux. It is computed using the following equation given for Landsat images-

Normalized Difference Vegetation Index (NDVI):
NDVI is an index that provides a standardized method of comparing vegetation greenness between satellite images. NDVI can be used as an indicator of relative biomass and greenness (Boone et al. 2000, Chen 1998.

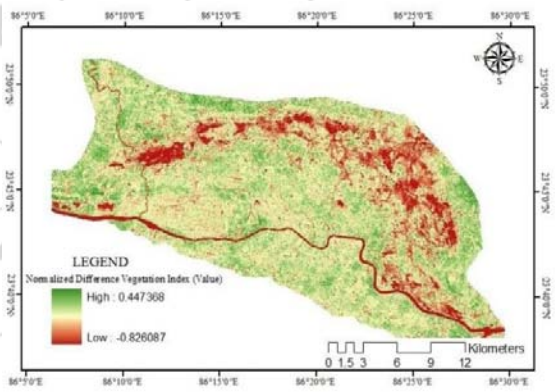

Figure 7: NDVI Map of Jharia Coal Field (2001)

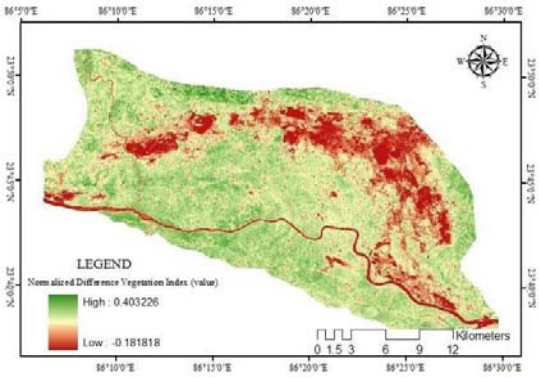

Figure 8: NDVI Map of Jharia Coal Field (2011)

NDVI are good indicators of photosynthetic activity on the vegetation surface. NDVI is the ratio of the differences in reflectivity for the near-infrared band (P_{nir})and the red band (P_{red}) to their sum:

$$NDVI= (P_{nir}- P_{red})/ (P_{nir}+P_{red})\text{……..} (7)$$

Where,

P_{nir} = reflectivity of band 3, Pred = reflectivity of band 4

Vegetation proportion

Proportion vegetation (pv) cover is a dynamic variable which changes on a daily basis, yet to this point most models simply include a climatologically value for the percent healthy vegetation cover. Remote sensing from satellites now provides enough detailed and continuous coverage of the Earth's surface to provide an indirect, NDVI-based vegetation cover product. Pv was used to separate non-vegetated, partially vegetated and densely vegetated land surfaces.

Pv= {(NDVI-NDVImin)/(NDVImax-NDVImin)}2

Where,

NDVI=Normalized Difference Vegetation Index (calculated equation-5)

NDVImax = NDVI value of full vegetation cover

NDVImin = NDVI value of bare soil.

Emissivity

The land surface emissivity widely varies with the land cover and the wavelength. For the rough estimation of the emissivity variation, the emissivity category is defined, to separate the spectral dependency and the magnitude of the emissivity. Thermal infrared emissivity is an important parameter both for surface characterization and for atmospheric correction methods. Mapping the emissivity from satellite data is therefore a very important question to solve. The main problem is the coupling of the temperature and emissivity effects in the thermal radiances. Several methods have been developed to obtain surface emissivity from satellite data. Emissivity calculated using following formula-

$$€=€veg.Pv+€Soil(1-Pv)u\text{……} (9)$$

Where,

€veg = the emissivity of vegetation, estimated as 0.99

€Soil = the emissivity of soil, estimated as 0.97

Pv = is the vegetative proportion (computed in equation-6)

Atmospheric Transmissivity

Atmospheric transmissivity is defined as the fraction of incident radiation that is transmitted by the atmosphere and it represents the effects of absorption and reflection occurring within the atmosphere. This effect occurs to incoming radiation and to outgoing radiation, Include transmissivity of both direct solar beam radiation and diffuse (scattered) radiation to the surface. We calculate assuming clear sky and relatively dry conditions using following equation-

$$R=0.75+2\times10\text{-}5\times z\text{……..}(10)$$

Where,

Z=elevation above mean sea level this elevation should best represent the area of interest, such as the elevation of the relevant weather station.

T=0.75+2*10-5*Z,

=0.75+2*10-5*170m

$$=0.77304\text{……} (11)$$

Thermal radiance at surface level:

At-sensor spectral radiance was then converted to surface-leaving radiance by using following equation (Yuan & Bauer, 2007),

$$LT=\frac{L\lambda-Lu-R(1-€Ld}{t€}\text{……}(12)$$

Where,

Lr=Radiance of the blackbody,

Lλ=Spectral radiance at sensor‟s aperture in W /(m2.sr.µm).

Lu=The radiation brightness upward from atmosphere 1.68 W /(m2.sr.µm)

Ld=The radiation brightness downward from atmosphere 1.74 W /(m2.sr.µm).

T=The atmospheric transmission, estimated as 0.77,

€=The emissivity of the surface, specific to the target type.

Land Surface Temperature:

The Radiance Was Converted To Surface Temperature Using The Following Equation. (Yuan & Bauer, 2007),

$$TR=k2/in(k1/LT+1)\text{…….}(.13)$$

Where,

TR= Temperature In Kelvin,

K1 & K2 = Calibration Constant,

LT= Spectral Radiance.

For Landsat-5 TM, K1 & K2 Was 607.76 & 1260.56 Respectively. And Landsat-7 ETM+, K1 & K2 Was 666.09 & 1282.71 Respectively.

LMIN and LMAX values for Landsat 5 TM (Left: for 1984 from Markham and Barker, 1986, Right: for 2000 calibrated by Univ. Idaho 2002):

Table 1: Land Surface Temperature

Band number	For 2000	
	W*m-2*ster-1*µm-1	
	LMAX	LMIN
1	178.941	-1.765
2	379.055	-3.576
3	255.695	-1.502
4	242.303	-1.763
5	30.178	-0.411
6	15.600	1.238
7	13.156	-0.137

Table 2: Land Surface Temperature

Band number	After 15, Jan, 1984	
	W*m-2*ster-1*µm-1	
	LMAX	LMIN
1	152.100	-1.500
2	296.800	-2.800
3	204.300	-1.200
4	206.200	-1.500
5	27.190	-0.370
6	15.600	1.238
7	14.380	-0.150

LMAX and LMIN values for Landsat 7 ETM+ (Landsat 7 Science User Data Handbook Chap.11, 2002)

Table 3: Land Surface Temperature

Band number	Before July 1,2000			
	W*m-2*ster-1*µm-1			
	Low Gain		High Gain	
	LMIN	LMAX	LMIN	LMAX
1	6.20	297.50	-6.20	194.30
2	-6.00	303.40	-6.00	202.40
3	-4.50	235.50	-4.50	158.60
4	-4.50	235.00	-4.50	157.50
5	-1.00	47.70	-1.00	31.60
6	0.00	17.04	3.20	12.65
7	-0.35	16.60	-0.35	10.932

Table 4: Land Surface Temperature

Band number	After July 1,2000			
	W*m-2*ster-1*µm-1			
	Low Gain		High Gain	
	LMIN	LMAX	LMIN	LMAX
1	-6.20	293.70	-6.20	191.60
2	-6.40	300.90	-6.40	196.50
3	-5.00	234.40	-5.00	152.90
4	-5.10	241.10	-5.10	157.40
5	-1.00	47.57	-1.00	31.06
6	0.00	17.04	0.00	12.65
7	-0.35	16.04	-0.35	10.80

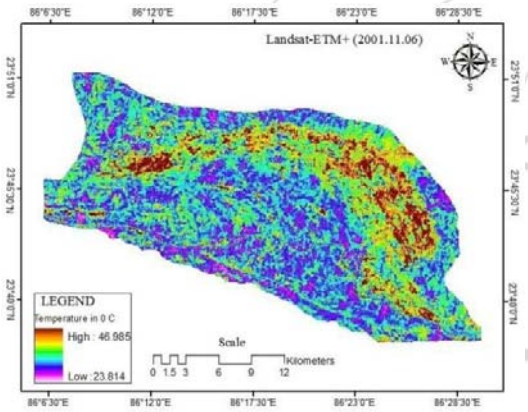

Figure 9: Temperature Map of Jharia Coal Field (2001)

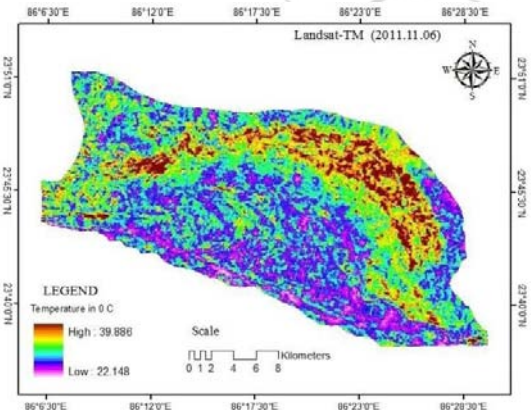

Figure 10: Temperature Map of Jharia Coal Field (2011)

6. Results & Discussion

In this study aimed to assess the status of coal mining area and coal fire in the Jharia coal field through period of 2000 and 2011 with the help of thermal infrared data. For identification coal fires & coal mining temperature used Landsat-5 TM & Landsat-7 ETM+ thermal data whose resolution 120m & 60m respectively. However, we have used Landsat-TM (morning) and Landsat-ETM+(noon) data for comparison of coal fire areas.

In Jharia coal field maximum temperature computed for the year 2000 from Landsat-ETM+ was 46 0c and for the year 2011 from Landsat- TM was 40 0c, as well as variation in spatial and spectral resolution in thermal region between to sensors of same satellite. The coal fire map produced for the years 2000 and 2011 depicts the pattern of coal fire in the Jharia coal field, present in figure-11 & figure-12 respectively.

According to coal fire map for the year 2000 & 2011 reveled that coal fires were mostly developed in eastern and western parts but mostly develop in eastern part of JCF. Coal fires were mainly restricted in Barakar Formation. Two major coal fire zones present in the eastern part of the Jharia coal field are the Lodna– Tisra–Kujama–Jiyalgarha and the Kusunda–Kenduadih zones. The most significant coal fire zone is Gonudih, present in western part of JCF. In Tisra, Kenduadih, Nadkhurkee areas pixel temperatures found >46 0C from Landsat- ETM+ data. The fire zone in the western part of the JCF was limited to the Dumra–Nadkhurkee–Jayramdih area.

It is reported that from two coal fire map, coal fire affected area increase for the year 2011 in eastern part of JCF in comparison to 2001(figure-11). The major collieries, which showed an increase in fire-affected area were Kusunda (0.56 km2), Golukdih (0.18 km2), Lodna (0.18 km2), South Jharia OCP (0.9 km2) etc. In contrast, the impact of fire had diminished considerably in collieries such as Nadkhurkee (0.35 km2), Godhar (0.14 km2), Benedih (0.11 km2), Gonudih (0.22 km2) and South Tisra (0.24 km2). The cause of the increase in total fire area in 2011 with respect to 2001 is due to the contribution from the Kusunda–Golukdih–Ena–Bastacolla area.

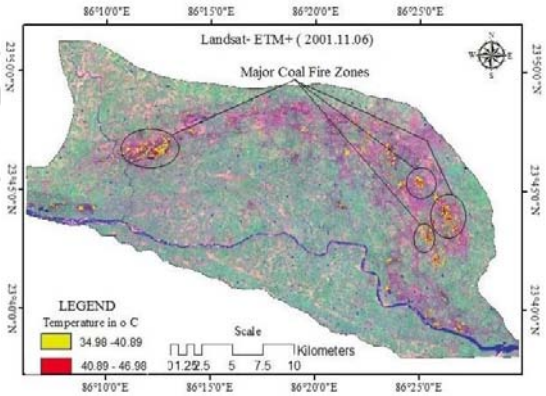

Figure 11: Coal fire map of Jharia coal field (2001)

Delineation of land surface temperature over Google Earth with help of Web-GIS techniques:

Some segment of Jharia coal field area has been cut with the help of Google Earth for the study of Land Surface Temperature (LST). At first raster temperature data has been converted into line vector layer for interpolation. Secondly Isothermal vector lines converted to KML file format. These

Isothermal lines are plotted over the Google Earth by Web-GIS techniques and visually interpreted.

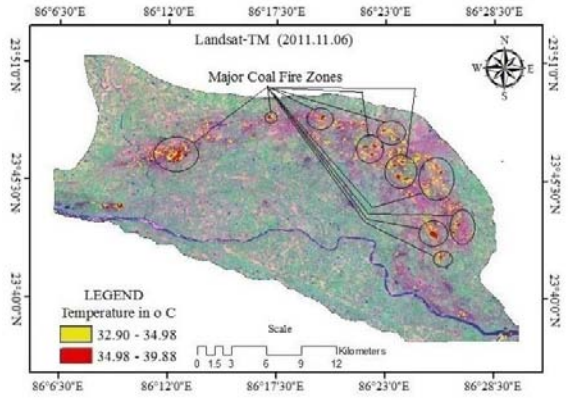

Figure 12: Coal fire map of Jharia coal field (2011)

According to figure-13, it is reported that maximum temperature present in coal mining area. Temperature found in Jharia mining area between 33°c to39°c. in vicinity of mining area temperature varies less than 29°c. In above two figures 14 and 15 it is clearly identified that coal mining areas are main high temperature zone, whose temperature varies greater than 33°c.

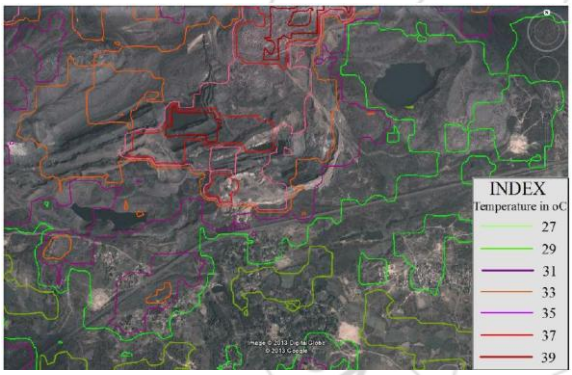

Figure 13: Maximum temperature present in coal mining area

When difference increase from mining area to forested area, temperature decreases rapidly. According to fig-14, maximum temperature is 37°c in Kustore mining area but difference increase to Amrapall forest, present in this area, temperature decrease to less than 27°C.

Figure 14: Maximum temperature present in coal mining area

Not only high temperature zone mining areas but also settlement areas are high temperature zone, these are made of cement, asbestos etc. it is clearly proved from fig-15, Kusunda mining area, temperature of settlement areas varies between 29°c to 33°c. Some vegetated land present in this area, whose temperature is less than 29°c.

7. Land Use / Land Cover in Jharia Coal Field Region

The array of information available on land use/cover requires be arranging or grouping under a suitable framework in order to facilitate the creation of database. Further, to accommodate the changing land use/vegetation cover pattern, it becomes essential to develop a standardised classification system that is not only flexible in nomenclature and definition, but also capable of incorporating information obtained from the satellite data and other different sources.

The present framework of land use/cover classification has been primarily based on the „Manual of Nationwide Land Use/ Land Cover Mapping Using Satellite Imagery" developed by National Remote Sensing Agency, Hyderabad, which has further been modified by CMPDI for coal mining areas. Land use/vegetation cover map was prepared on the basis of image interpretation carried out based on the satellite data for the year 2000 & 2011 through the help of Landsat-TM & Landsat-ETM+ satellite images. Following land use/cover classes are identified in the Jharia coalfield region-

- **Mine dump:** those areas where waste debris is dumped before and after extraction of coal.
- **Mining area:** those areas presently under coal mining activity.
- **Ash pond:** including small areas where waste materials are stored and surface water is collected inside this area during the operational phase of the mine.
- **Agricultural land:** land under cultivation where various types of agricultural activities are practised.
- **Agricultural land (fallow):** lands taken up for cultivation but temporarily allowed to rest, uncropped for one or more seasons, but not less than one year.
- **Built-up area:** areas where human settlements exist at present.
- **River/Water body:** areas filled with water.
- **River sand:** sand deposit on the banks of the Damodar River.
- **Open scrub:** areas with sparse vegetation or devoid of scrub and with a thin soil cover.
- **Barren land (rocky):** rock exposures, often barren and devoid of soil and vegetation. These areas are found wherever Raniganj sandstones are exposed.
- **Barren land:** barren lands without vegetation and rocky exposure.
- **Forest plantation:** areas where afforestation has been carried out mainly for environmental hazard control.
- Forest land: lands that have been protected as forest land.

Land use & land cover pattern in Jharia coal field area: Management of Land use & land covers are the important parameter for controlling environmental degradation. Due to need for their life land use/land cover change. In Jharia coal field (JCF) area major economical source is production of coal. For this resion increase coal mining area which effects

on forest area, agriculture land etc. agriculture land reduce and increase fallow land due to fly ash come from mining area. Due to same cause forested area reduce and increase scrub land. For change detection analysis multi-temporal satellite data needed, in this study we use Landsat-TM (2011) & Landsat-ETM+ (2001) satellite data for time sequential change of two years. Land use & land cover map for the years 2001 & 2011 present in figure-16 & figure-17 respectively. According to land use/ land cover classification for the year 2000, it is revealed that in JCF region mostly covered by barren land, fallow land (agriculture) and coal mining area.Barren land found in north-wastern, southern part, north-eastern & middle part. Fallow land found in vicinity of coal mining areas. Coal mining area found in eastern & western part of this region. Damodar is the One major river of this area, present in lower of JCF & three minor rivers these are- Jamunia nadi, Khudia nadi, & Katri nadi respectively joint with Damodar river. Some agriculture land mostly present in north-western part, middle part and dense vegetation & scrub land present eastern & south-eastern part, middle portion of Jharia coal field. Total area of land use/ land cover and % of each class present in table-7

Table 5: Land use / land cover area in Jharia coal field (2001)

Sl. No.	Class Name	Area in hector	Area in %
1	Settlement	906.95	1.565
2	Barren land	10189.07	17.589
3	Agriculture land	5189.065	8.958
4	Scrub land	6840.28	11.808
5	Water body	1154.85	1.994
6	River sand	219.226	0.378
7	Fallow land	20288.21	35.023
8	Mining area	6837.19	13.39
9	forest	4381.85	9.29
	Total Area	57927.42	100

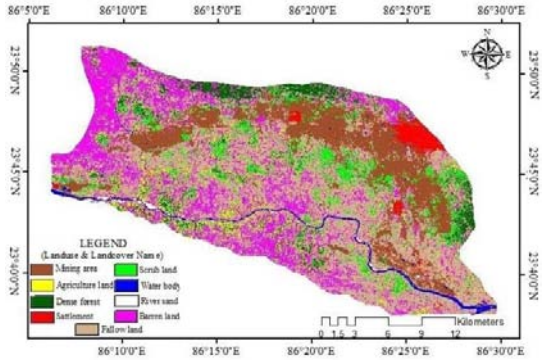

Figure 15: LULC Map of Jharia Coal Field(2001)

Table 6: Land use / land cover area in Jharia coal field (2011)

Sl. No.	Class Name	Area in hector	Area in %
1	Settlement	1206.72	2.08
2	Barren land	11777.04	20.38
3	Agriculture land	2463.21	4.25
4	Scrub land	4112.01	7.1
5	Water body	919.98	1.59
6	River sand	483.93	0.84
7	Fallow land	22745.61	39.27
8	Mining area	10565.461	18.24
9	forest	3653.46	6.31
	Total Area	57927.42	100

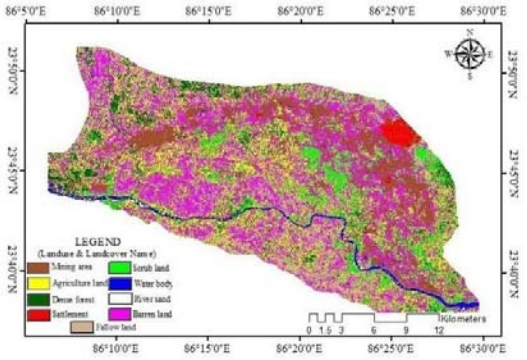

Figure 16: LULC Map of Jharia Coal Field (2011)

According to figure-16, land use & land cover map of Jharia coal field for the year 2011, it is revealed that fallow land, barren land & coal mining area these are major classes of this area. Barren land found western & north-western part and southern part of this area. Fallow land found in eastern & middle portion of this area and coal mining area extended from east to west direction of JCF. Some spar vegetated land & scrub land present in northern, eastern & middle portion of study area. Jamuniya, khudia, karti these are minor river join with Damodar river, main rivers of this coal basin. Some agriculture land found in lower, basically both side of Damodar river and settlement found in north-eastern part, eastern area basically Jharia, some part of Dhanbad area. Details land use/ land cover area and % of each classes present in the table-

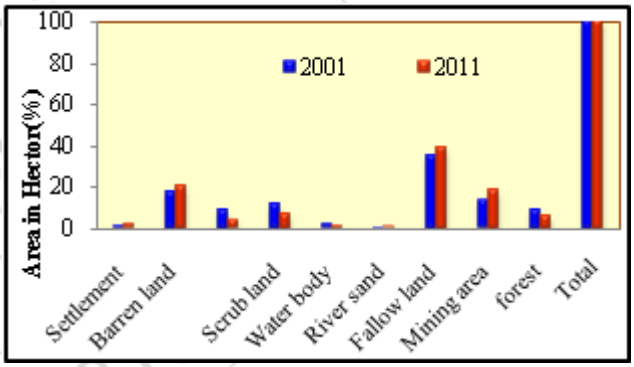

Figure 17: Various LULC of two different years of JCF

Table 7: Changing land use / land cover area in Jharia coal field (2001 to 2011)

Settlement	1.565659	2.083159	0.52
Barren Land	17.58928	20.33068	2.74
Agricultural Land	8.957832	4.252235	-4.71
Scrub Land	11.80831	7.098555	-4.71
Water body	1.993618	1.58816	-0.41
River Sand	0.378437	0.835407	0.46
Fellow Land	35.02334	39.26571	4.24
Mining Area	13.3929	18.23913	4.85
Forest	9.290626	6.306961	-2.98
Total	100		

Table-7 represents rate of change in area of different LULC classes over time. Different types of land use & land cover present, but some classes increase and some classes reduce.

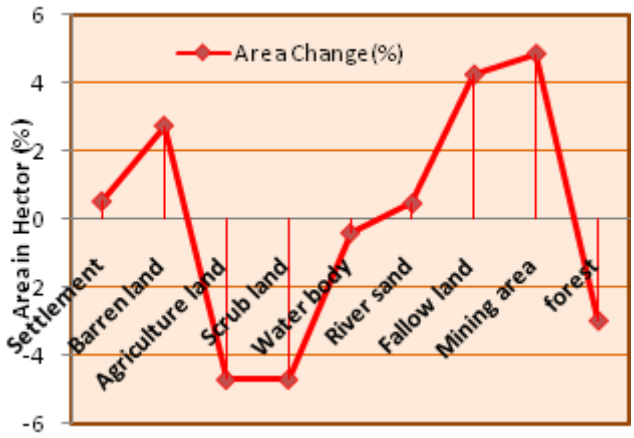

Figure 18: Graphical representation of various LULC changes of Jharia coal field (2001-2011)

Increase coal mining area 4.87% of Jharia coal field, but forested land & scrub land reduce 2.98 % & 4.71 % respectively. Heavy changes of total vegetated land indicate deforestation and natural degradation. Agriculture lands have reduced and fallow land increase from 2001 to 2011. Total agriculture land change -4.71%, highly negative value. Due to increase coal fire zone and it produce many by-products like ash, which effects on agriculture land and reduce crop product. Finally reduce agriculture land increase fallow land. Total increase fallow land 4.23% of 10 years periods and its related barren land change 2.74% of Jharia coal field. Settlement, river sand, water body has been minor changes. Details change of various land use & land cover classes present in figure-18.

8. Conclusion

The Landsat-TM & ETM+ thermal remote sensing data were used to estimate coal-fire temperature and the threshold temperatures were determined using a knowledge-based iterative technique to delineate the coal-fire and non-coal-fire areas. A good knowledge of local geology is used to interpret and differentiate the coal fire induced anomalies more accurately from some low thermal inertia rocks. The results also shows use of NDVI derived emissivity can return a more reliable temperature rather than use of a standard emissivity for all types of land cover.In the year 2001, the eastern part of the Jharia coal field was more affected by coal fire than the western part. The same situation was continued in the year 2011. Hence, the eastern part is always affected by the coal fire. An increase (1.67 km2) in the total coal-fire area was observed from 2001 to 2011. Major collieries affected by coal fire are Kusunda, Kujama, Bararee and Ena. Largescale mining of coal in these collieries has accelerated the fire movement by allowing fire to become in contact with oxygen, thereby allowing faster propagation to occupy a large areal extent. The Nadkhurkee fire is controlled by dumping fine-grained fly ash over the fire zone in order to stop the supply of oxygen. The cause of the increase in fire in the Shatabdi area could be due to the presence of faults and fractures, which play an important role by allowing ambient oxygen to remain in contact with the fire.

The land-use/land-cover map prepared from Landsat-TM & ETM+ data for time sequential change of LULC patters. Mining area rapidly increase day to day, total increase mining from 2001 to 2011 is 4.85%. There are some human settlements present close to mining- and fire-affected areas. This poses serious health problems for the local inhabitants. Rail track has been removed completely for safety reasons in some places. Hence, the topography has to be managed well to improve the environmental condition of the Jharia coal field.

References

[1] Bhattacharya, A. and Reddy, C.S.S., 1995, Inventory and monitoring of underground and surface coal mine fire in Jharia coalfield, Bihar using thematic mapper thermal IR data. A report by Geosciences Group, National Remote Sensing Agency, Hyderabad, India, Report no. NRSA-AD-GG-TR-2/95

[2] Cassells, C. J. S., van Genderen, J. L., and Zhang, X. M., 1996, Detecting and measuring underground coal fires by remote sensing, Proceedings of the 8th Australian Remote Sensing Conference, Canberra, March 1996, Volume II, Thursday 28-3-96, pp. 90- 101.

[3] Fisher, W., and Knuth, W. K. jr., 1968, Detection and delineation of subsurface coal fires by aerial infrared scanning, Geological Society America Special Paper,vol-115, p. 67- 68.

[4] Gangopadhyay, P.K., 2003, Coal fire detection and monitoring in Wuda, North China, A multispectral and multi-sensor approach, M.Sc. dissertation, International Institute for Geo-Information Science and Earth Observation (ITC), Enschede, The Netherlands.

[5] Gangopadhyay, P.K., Maathuis, B. and Van Dijk, P., 2005, ASTER derived emissivity and coal-fire related surface temperature anomaly a case study in Wuda, North China. International Journal of Remote Sensing, vol-26, pp. 5555–5571.

[6] Gupta, R. P., and Prakash, A., 1998, Refectance aureoles associated with thermal anomalies due to subsurface mine fires in the Jharia coal field, India. International Journal of Remote Sensing, 19, 2619-2622.

[7] LANDSAT 7 SCIENCE DATA USERS HANDBOOK, 2008, Level 1G product–band 6 conversion to temperature (accessed 15 May 2008).

[8] Mansor, S. B., Cracknell, A. P., Shilin, B. V., and Gornyi, V. I., 1994, Monitoring of Underground coal fires using thermal infrared data. International Journal of Remote Sensing, vol-15, 1675-1685.

[9] Prakash, A., Gupta R. P., and Saraf, A. K., 1997, A Landsat TM based comparative study of surface and subsurface fires in the Jharia coal field, India. International Journal of Remote Sensing, vol-18, 2463-2469.

[10] Prakash, A., Saraf, A. K., Gupta, R. P., Dutta, M., and Sundaram, R. M., 1995a, Surface thermal anomalies associated with underground fires in Jharia coal mines, India, International Journal of Remote Sensing, vol-16, 2105-2109.

[11] Prakash, A., Sastry, R. G. S., Gupta, R. P., and Saraf, A. K., 1995b, Estimating the depth of buried hot feature from thermal IR remote sensing data, a conceptual approach. International Journal of Remote Sensing, vol-16, 2503-2510.

[12] Prasad, S. N., Rao, M. N. A., and Mookherjee, A., 1984, Mine planning a step towards modernization, Coalmining in India, 12th World Mining Congress New Delhi, Internal Publication, (Ranchi, CMPDIL)
[13] Reddy, C.S.S., Srivastav, S.K. and Bhattacharya, A., 1993, Application of Thematic Mapper short wavelength infrared data for the detection and monitoring of high temperature related geoenvironmental features. International Journal of Remote Sensing, vol-14, pp. 3125–3132.
[14] Rosema, A., Genderen, J. L. van, and Schalke, H. J. W. G., 1993, Environmental monitoring of coal fires in North China. Project Identification Mission Report October 1993, BCRS report 93-29, The Netherlands, pp. 18-19.
[15] Saraf, A.K., Prakash, A., Sengupta, S. and Gupta, R.P., 1995, Landsat-TM data for estimating ground temperature and depth of sub-surface coal fire in the Jharia coalfield, India, International Journal of Remote Sensing, vol-16, pp. 2111–2124.
[16] Saxena, N.C., 2002, Jharia Coalfield Today, Tomorrow and Thereafter, MIENVIS News Letter, vols. 33–34 (Dhanbad, Jharkhand: Centre of Mining Environment, Indian School of Mines), ISSN 0972–4648.
[17] Van De Griend, A.A. and Owe, M., 1993, On the relationship between thermal emissivity and the normalized difference vegetation index for natural surfaces. International Journal of Remote Sensing, vol-14, pp. 1119–1131
[18] YamaguchI, Y., Kahle, A.B., Tsu, H., Kawakami, T. and Pniel, M., 1998, Overview of Advanced Spaceborne Thermal Emission and Reflection Radiometer (ASTER).IEEE Transactions on Geoscience and Remote Sensing, vol-36, pp. 1062–1071
[19] Zhang, J.,Wagner, W., Prakash, A.,Mehl, H. and Voigt, S., 2004, Detecting coal fires using remote sensing techniques. International Journal of Remote Sensing, vol-25, pp. 3193–3220.